Numerical Study of Suction Injection Driven Nanofluid Through Parallel Plates Channel

Hina Bashir, Huma Gull, Azra Aziz, Bisma Imran

Department of Mathematics & Statistics, University of Southern Punjab, Multan, Pakistan

Abstract: The main purpose of this research is to analyze the effects of nanofluids that are based on the injection and suction parameters, where the channel is structured using parallel plates. For making governing PDEs dimensionless, we use similarity transformations to convert them into a system of coupled nonlinear ODEs. These ODEs are solved by applying the method of Quasi-Linearization, and on the other hand, structural derivatives are approximated by using the central difference technique. The effects of employing parameters on temperature and velocity are graphically studied. During the injunction, mass transfer decreases and increases in the case of suction transfer rate of heat and mass for the Reynolds number.

Keywords: Nanofluid, Injection/Suction, Reynolds' Number.
Email: humagull@isp.edu.pk

1. Introduction

The noteworthiness of magneto-hydrodynamics (MHD) flow of nano-fluid over curved stretching sheet has been seen in the field of structural engineering. The flow of such MHD fluids over a stretchable curved sheet is studied scientifically due to many characteristics regarding heat transfer and fluid by using the R-K method, Choi [1]. In the circulatory system, blood flows hydrodynamically under the influence of a magnetic field studied by Abbasi [2]. Hayat [3] considered the curved surface for heat transfer, studied regarding magnetic properties, while Cortell [4] studied a curved sheet with the help of heat production of the stagnation point. Also, Hussain [5] discussed mixed gathering flow with low dissipation of a micro-polar fluid over a stretching surface. He also got the result of the deferment and infusion solution by using the 5^{th}-order Runge-Kutta-Feldberg method. The MHD flow of a micro polar fluid has been dealt with through porous medium, and the prevailing equations are studied scientifically, Abbas [6]. Sajid [7] described the nonlinear results of a stretchable surface with transfer of heat and mass fixed in a spongy medium of hydrodynamic flow. Sandeep [8] described chemical properties and results of a spongy surface of a magneto-hydrodynamic flow with the help of a mathematical method, while major properties of a curved plate are discussed by Lee [9]. Helal [10] described the micro-polar fluid of hydro-magnetic and warmth convection over a vertical plate. Also, Kumar [11] debated the results of steady magneto-hydrodynamic flow of micro-polar fluid over a stimulating surface and the effect of heat creation and secretion as well. Quasim [12] discussed relocating the mass and warmth possessions on an elongating surface, while mass and warmth possessions of micro polar fluid with thermal emission on shaky MHD flow were described by Hayat [13-14]. Khan [15] examined the injection/suction constraint and instability of the parameter analytically. Hayat et al. [16] studied rotating flow of a micro-polar fluid over an overhanging sheet, while Nadeem [17] presented MHD flow mathematically by using the constrained element method over a curved sheet. Khairy [18] discussed graphically the consequence of the slip parameter on the stream of a curved surface. Khan [19], defined geophysical applications as upgrading in oil recovery, geothermal tanks, cooling of nuclear reactor and thermal padding while Kumar [20], worked on 2 dimensional steady micro polar incompressible fluid flow at a stationary point over a curved sheet, also increase in boundary layer of dimensionless twist causes are numerically answered by using Runge Kutta(R-K) method. By using the same mathematical formulation, more results are obtained for micro-polar fluid over a curved surface, Makinde [21].

2. Mathematical Formulation

We suppose a 2-D steady, laminar, and adhesive hydromagnetic fluid. The flow of this fluid through parallel plates, whose lower plate is in contracting form while the upper plate is at rest, and all this setup is surrounded by a magnetic field which is applied transversally. The applied magnetic field is of negligible strength compared to the imposed magnetic field. The Reynolds number is the ratio between the product of the characteristics of length and velocity of fluid, and the diffusivity of the magnetic field. The value of the Reynolds number is supposed to be very small and is employed to measure the strength of magnetic field lines through the conducting fluid. Such Reynolds numbers exhibiting the trend of magnetic field are directed outward, which is a representation of a purely diffusive state. Further, we suppose that no external polarization force is imposed, and as a consequence, no electric field is present. Body forces are assumed to be absent. The channel wall is located at $y = -a$, and the other is at $y = a$. A cross section of the channel is $2a$. Velocity and micro rotation are in the following form.

$$\underline{\boldsymbol{v}} = (\boldsymbol{u}(\boldsymbol{x},\boldsymbol{y}), \boldsymbol{v}(\boldsymbol{x},\boldsymbol{y}), \boldsymbol{0}), \quad \underline{\boldsymbol{v}} = (\boldsymbol{0}, \boldsymbol{0}, \boldsymbol{\varphi}(\boldsymbol{x},\boldsymbol{y})) \tag{1.1}$$

Whereas, φ is the normal component of microrotation to $the\ xy$-plane.

$$\frac{\partial \boldsymbol{u}}{\partial \boldsymbol{x}} + \frac{\partial \boldsymbol{v}}{\partial \boldsymbol{y}} = \boldsymbol{0}$$

$$\frac{-\boldsymbol{1}}{\boldsymbol{\rho_{nf}}}\frac{\partial \boldsymbol{p}}{\partial \boldsymbol{x}} + \frac{\boldsymbol{\mu_{nf}}}{\boldsymbol{\rho_{nf}}}\boldsymbol{\nabla}^2\boldsymbol{u} = \boldsymbol{u}\frac{\partial \boldsymbol{u}}{\partial \boldsymbol{x}} + \boldsymbol{v}\ \frac{\partial \boldsymbol{u}}{\partial \boldsymbol{y}}$$

$$\frac{-1}{\rho_{nf}}\frac{\partial p}{\partial y}+\frac{\mu_{nf}}{\rho_{nf}}\nabla^2 v = u\frac{\partial v}{\partial x}+v\,\frac{\partial v}{\partial y} \tag{1.2}$$

$$\rho_{nf}C_p\left(uT_x+vT_y\right)=k_0T_{yy}+\mu_{nf}(u_y)^2$$

Where ρ_{nf} and μ_{nf} are the density and viscosity of the nano fluid. Moreover, p, T, k_o, and C_p represent the pressure, temperature, thermal conductivity, and specific heat at constant pressure, respectively. The constraints on temperature and the temperature field are

$$T(x,a)=T_2,\qquad T(x,-a)=T_1,\qquad v(x,a)=0,\qquad v(x,-a)=\tau_\omega, \tag{1.3}$$

$$u(x,-a)=-bx,\qquad u(x,a)=0$$

Here, the temperatures of the lower and upper walls of the channel are T_1 and T_2, respectively, where $T_2 < T_1$. $b > 0$ represents the rate of shrinking of the wall. If τ_ω is greater than zero, it is called the injection velocity, and if τ_ω is less than zero, it represents the suction velocity. We use similarity transformations to obtain ODEs from PDEs given in equation (1.2).

$$u=bxf'(\eta),\qquad v=-abf(\eta),\qquad \eta=\frac{y}{a},\qquad \theta(\eta)=\frac{T-T_2}{T_1-T_2} \tag{1.4}$$

$$\mu_{nf}=\frac{\mu_f}{(1-\varphi)^{2.5}}\rho_{nf}=(1-\varphi)\rho_f+\varphi\rho_s$$

Eliminating the pressure term from the momentum equations and applying the similarity transformation to the above equations, reduces to the equation

$$f^{(iv)}+Re(1-\varphi)^{2.5}\left((1-\varphi)+\frac{\rho_s}{\rho_f}\varphi\right)[ff'''-f'f'']=0 \tag{1.5}$$

Equation (1.4) is transformed into the following equation after employing similarity transformations

$$\theta''+\left((1-\varphi)+\frac{\rho_s}{\rho_f}\varphi\right)\mathrm{Re}\,\mathrm{Pr}\,f\theta'+\frac{1}{(1-\varphi)^{2.5}}\mathrm{Ec}\,\mathrm{Pr}\,f''^2=0 \tag{1.6}$$

$$f'(a)=0,\qquad f'(-a)=1,\qquad f(a)=0,\qquad f(-a)=A_\omega,$$

$$\theta(a)=0,\qquad \theta(-a)=1 \tag{1.7}$$

where $Re=\frac{a^2b\rho_f}{\mu_f}, Pr=\frac{\mu_fC_p}{k_0}, Ec=\frac{(bx)^2}{C_p\Delta T}$ are Reynolds, Prandlt and Eckert numbers respectively and $\Delta T=T_1-T_2$. $A_\omega=-\frac{\tau_\omega}{ab}$ is called the parameter of suction when $A_\omega>0$, and when $A_\omega<0, it\ is$ called the injection parameter.

3. Result and Discussion

In this paper, we considered the effects of suction and injection parameters on the flow of nano-fluid on parallel plates. The ordinary differential equations (1.5) and (1.6), along with equation (1.7), are numerically solved by applying linearization of FDM with fixed values $\varphi = 0.08, Pr = 0.1, and\ Re = 5$. During the injunction, the tangential and normal velocity decreases, and on the other hand, the field behaved in the opposite direction. (Fig. 1.1, 1.2, 1.3). As we increase the magnetic field tangential velocity decreases in injection while increases in lower plate and decreases in upper plate in case of suction (Fig. 1.4). Normal velocity decreases in lower plate and increases in upper plate in case of injection but in case of suction velocity increases in both (upper and lower) plates and decreases in the mid of channel (Fig 1.5). As we increase the Reynolds number, tangential velocity increases in injection and suction, but normal velocity behaves similarly (increases in the lower plate and decrease in upper plate) in injection and suction (Fig. 1.6, 1.7). The temperature field increases in case of injection and decreases in suction (Fig. 1.8). In case of injection, the temperature field increases in the upper channel while in case of suction, it increases in the lower channel and decreases in the upper channel while enhancing the Prandtl's number (Fig. 1.9). (Table 1) Shows that as we decrease values of injection parameter mass transfer decreases while heat transfer increases in lower part of the channel and decreases in upper part of the channel while (Table 5) present exactly opposite results as we enlarge suction parameter. The effect of magnetic field in injection shows that mass transfer decreases in lower part of the plate and increases in upper part of the plate while increases in case of suction and heat transfer behaved same in both injection/suction parameter (Table 2, 6) but (Table 3) express that in case of injection mass and heat transfer increase in lower channel and decrease in upper channel as Reynold's number increases but in case of suction heat and mass transfer increases in both channels (Table 7). In case of injection, heat transfer increases in the lower channel and decreases in the upper plate as Prandtl number increases (Table 4), while heat transfer increases in the case of suction (Table 8).

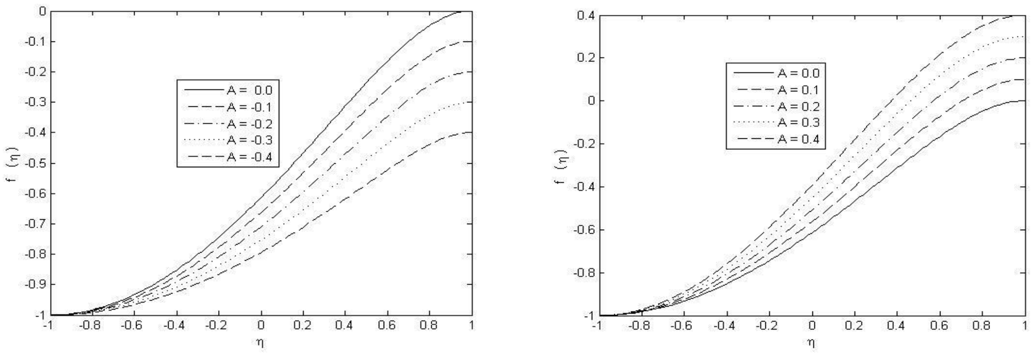

Figure 1.1 Tangential velocities of injection and suction parameters

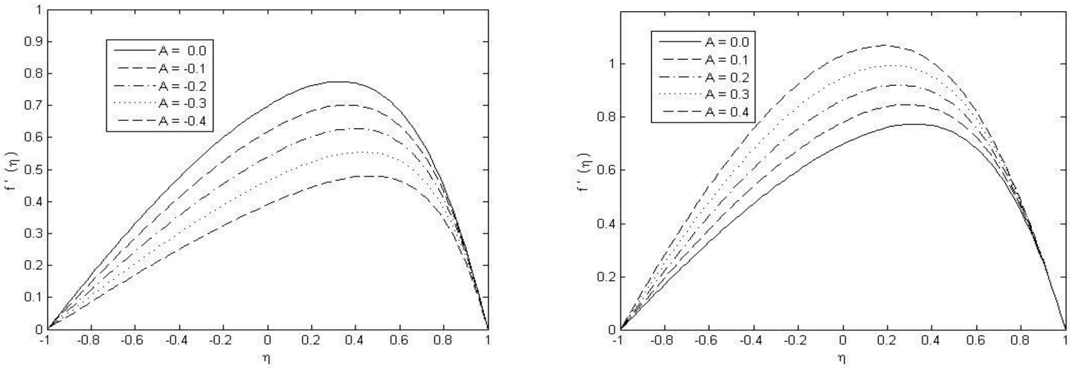

Figure 1.2 Normal velocities of injection and suction parameters

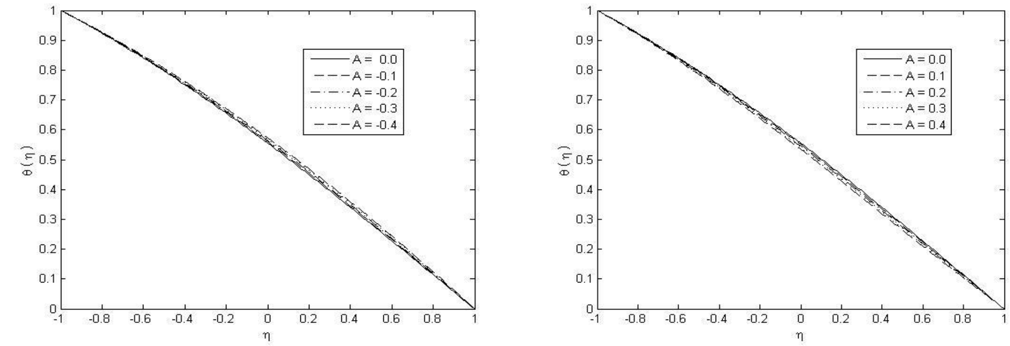

Figure 1.3 Temperature fields of injection and suction parameters

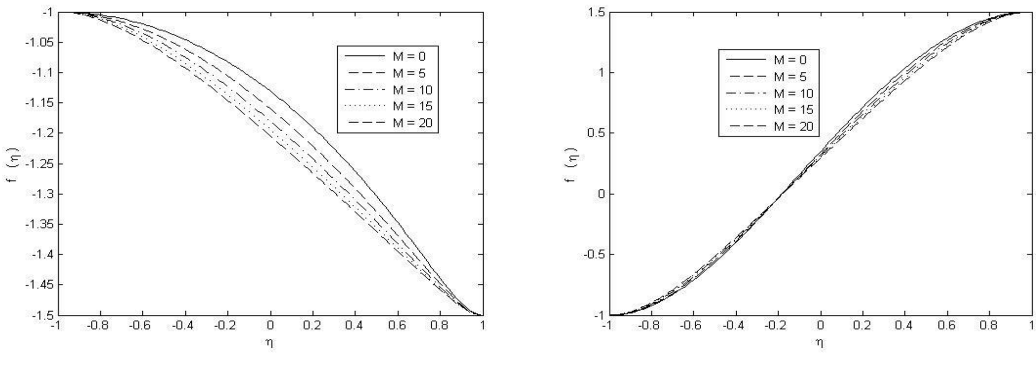

Figure 1.4Tangential velocities of injection and suction parameters

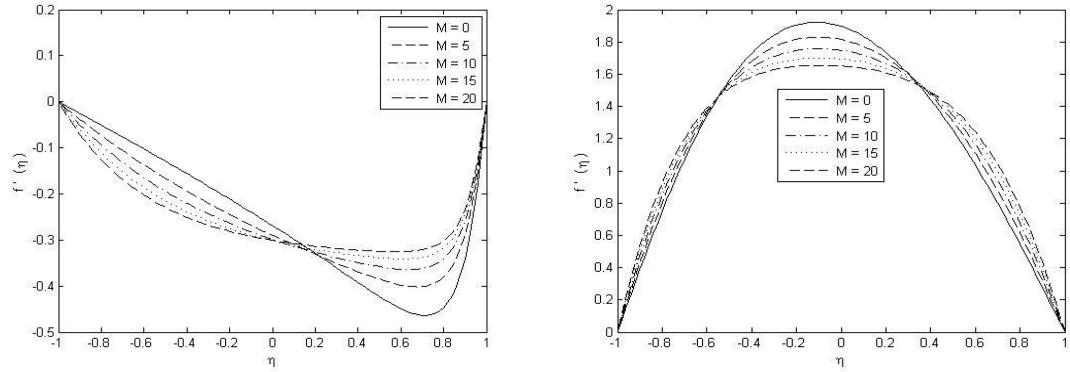

Figure 1.5 Normal velocities of injection and suction parameters

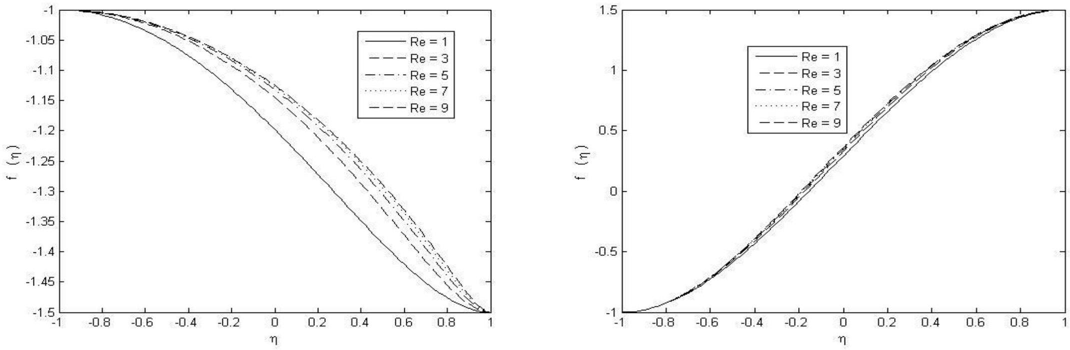

Figure 1.6 Tangential velocities of injection and suction parameters

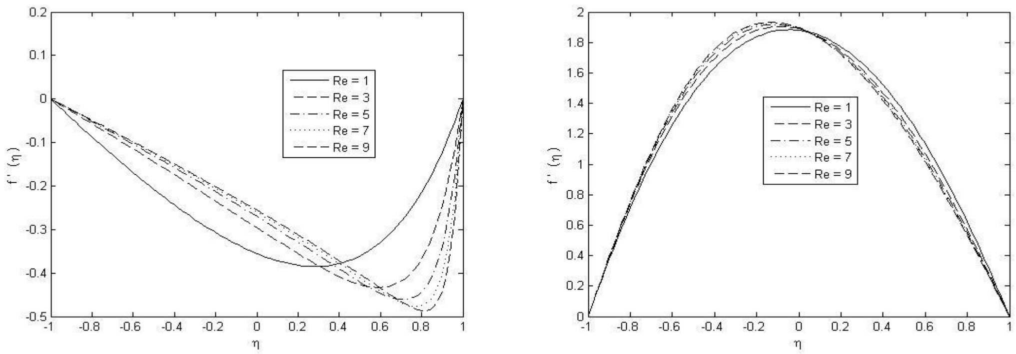

Figure 1.7 Normal velocities of injection and suction parameters

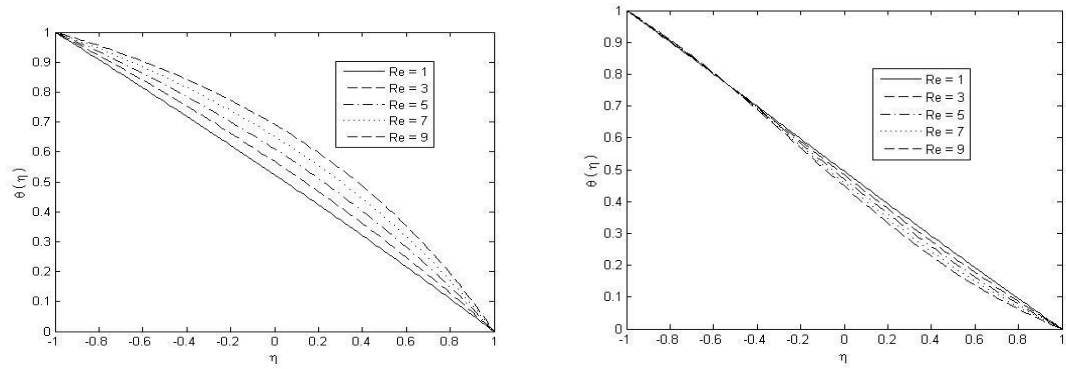

Figure 1.8 Temperature fields of injection and suction parameters

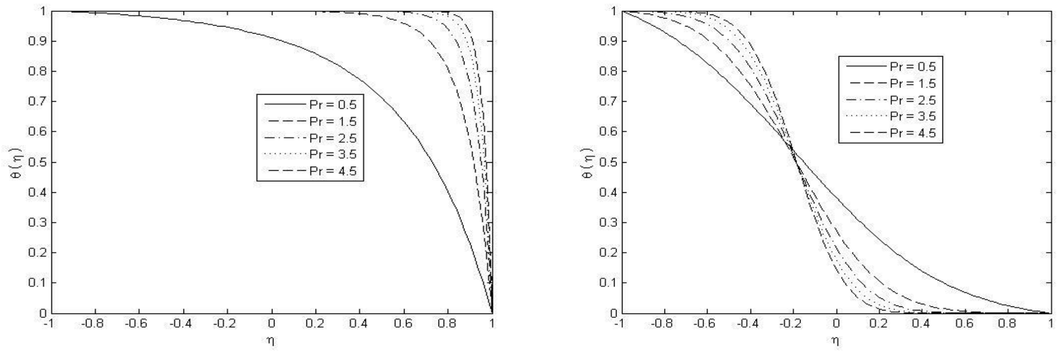

Figure 1.9 Temperature fields of injection and suction parameters

Tables for Injunction Parameters				
Table: 1				
For $R_e = 5, P_r = 0.1, and\ \phi = 0.08$				
A	$\theta'(-1)$	$\theta(1)$	$f''(-1)$	$f''(1)$
0.0	-0.370543	-0.370543	0.868962	-200.801078
-0.1	-0.365883	-0.585287	0.748101	-200.801754
-0.2	-0.361433	-0.600155	0.636766	-200.803044
-0.3	-0.357188	-0.614966	0.534208	-200.805115
-0.4	-0.353139	-0.629703	0.439649	-200.808165
Table: 2				
For $R_e = 5, P_r = 0.1, and\ \phi = 0.08$				
M	$\theta'(-1)$	$\theta'(1)$	$f''(-1)$	$f''(1)$
0	-0.318387	-0.786488	-0.253472	-54.622486
5	-0.316176	-0.791257	-0.391239	-54.618811
10	-0.314588	-0.794398	-0.526074	-54.616819
15	-0.313437	-0.796506	-0.653508	-54.615742
20	-0.312585	-0.797958	-0.772414	-54.615171
Table: 3				
For $R_e = 5, P_r = 0.1, and\ \phi = 0.08$				
R_e	$\theta'(-1)$	$\theta'(1)$	$f''(-1)$	$f''(1)$
1	-0.458005	-0.552546	-0.450289	-54.605317
3	-0.383618	-0.663606	-0.285524	-54.614073
5	-0.318283	-0.786719	-0.258928	-54.622283
7	-0.261324	-0.922887	-0.249985	-54.629243
9	-0.212381	-1.071702	-0.245534	-54.635102
Table: 4				

For $R_e = 5, P_r = 0.5, and\ \phi = 0.08$		
P_r	$\theta'(-1)$	$\theta'(1)$
0.5	-0.028623	-2.641685
1.5	-0.007066	-8.384369
2.5	-0.000235	-14.020445
3.5	-0.000006	-19.471428
4.5	0	-24.720939

Tables for Suction Parameters				
Table: 5				
For $R_e = 5, P_r = 0.1, and\ \phi = 0.08$				
A	$\theta'(-1)$	$\theta'(1)$	$f''(-1)$	$f''(1)$
0.0	-0.370543	-0.570387	0.868962	-200.801078
0.1	-0.375414	-0.555483	1.000034	-200.800847
0.2	-0.380494	-0.540613	1.141902	-200.800913
0.3	-0.385774	-0.525814	1.295024	-200.799464
0.4	-0.391244	-0.511126	1.459711	-200.799751
Table: 6				
For $R_e = 5, P_r = 0.1, and\ \phi = 0.08$				
M	$\theta'(-1)$	$\theta'(1)$	$f''(-1)$	$f''(1)$
0	-0.459904	-0.364796	3.998343	-200.797431
5	-0.459569	-0.366991	4.535631	-200.787545
10	-0.459459	-0.368714	5.043211	-200.778266
15	-0.459470	-0.370101	5.521787	-200.76955
20	-0.459547	-0.371242	5.973472	-200.761349
Table: 7				
For $R_e = 5, P_r = 0.1, and\ \phi = 0.08$				
R_e	$\theta'(-1)$	$\theta'(1)$	$f''(-1)$	$f''(1)$
1	-0.491169	-0.471089	3.913268	-208.49141
3	-0.475363	-0.415453	4.012514	-200.794335
5	-0.459885	-0.364896	4.020385	-200.797025
7	-0.444180	-0.319672	4.007698	-200.798379
9	-0.428220	-0.279462	3.991886	-200.799178
Table: 8				
For $R_e = 5, P_r = 0.5, and\ \phi = 0.08$				

P_r	$\theta'(-1)$	$\theta'(1)$
0.5	-0.028623	-2.641685
1.5	-0.007066	-8.384369
2.5	-0.000235	-14.020445
3.5	-0.000006	-19.471428
4.5	0	-24.720939

4. Conclusion

In this research, we discussed how the injunction and suction are affected by the magnetic field, Prandtl and Reynold numbers in a channel of parallel plates using similarity transformation. In case of suction, the velocity and temperature profiles are enhanced by enhancing the impact of the magnetic field, the Reynolds number, and the Prandtl number, respectively. While the temperature field increases in the lower part of the channel and decreases in the upper part of the channel, in the case of injection.

References

[1]. S.U.S. Choi, Eastman, J.A. Enhancing thermal conductivity of fluids with nanoparticles. *International mechanical engineering congress and exhibition, San Francisco, CA (United States)*, 12-17, (1995).

[2]. F.M. Abbasi, S.A. Shehzad, T. Hayat, A. Alsaedi, A. Mustafa, A. Obid, "Influence of heat and mass flux conditions in hydromagnetic flow of Jeffrey nanofluid", *AIP Adv*., 5(3) 037111, (2015).

[3]. T. Hayat, Z. Abbas, M. Sajid, "Series solution for the upper-convected Maxwell fluid over a porous stretching plate", *Phys. Lett. A*., 358(5-6) 396—403, (2006).

[4]. R. Cortell, "Heat and fluid flow due to non-linearly stretching surfaces", *Applied Mathematics and Computation*, 217(19) 7564—7572, (2011).

[5]. T. Hussain, SA. Shehzad, T. Hayat, A. Alsaedi, F. Al-Solamy, M. Ramzan, "Radiative Hydromagnetic Flow of Jeffrey Nanofluid by an Exponentially Stretching Sheet", *PLoS ONE*, 9(8) e103719, (2014).

[6]. T. Hayat, Z. Abbas, M. Sajid, "MHD stagnation-point flow of an upper-convected Maxwell fluid over a stretching surface", *Chaos Solitons & Fractals*, 39(2) 840—848, (2009).

[7]. T. Hayat, M. Sajid, "Analytic solution for axi-symmetric flow and heat transfer of a second grade fluid past a stretching sheet", *Int. J, Heat Mass Transf*., 50 75—84, (2007).

[8]. N. Sandeep, C. Sulochana, "Dual solutions for unsteady mixed convection flow of MHD micro polar over a stretching/shrinking sheet with non-uniform heat source/sink", *Int. J. Eng. Sci. Technol*., 18 (4) 738—745, (2015).

[9]. N.S. Akbar, S. Nadeem, C. Lee, “Characteristics of Jeffrey fluid model for peristaltic flow of chyme in small intestine with magnetic field”, *Results Phys.*, 3 152—160, (2013).

[10]. M. M. Helal, M.A. Saif, “Free convection heat and mass transfer in a power law fluid past an inclined surface with thermophoresis”, *J. Egypt. Math. Soc.*, 21 (3), 224--232 (2013).

[11]. N. Sandeep, B. Rushi Kumar, M. S. Jagadeesh Kumar, “A comparative study of convective heat and mass transfer in non-Newtonian nano-fluid flow past a permeable stretching sheet”, *Journal of Molecular Liquids*, 212, (2015).

[12]. M. Quasim, “Heat and mass transfer in Jeffrey fluid over stretching sheet with heat source/sink”, *Alex. Eng. J.*, 52(4), 571--575 (2013).

[13]. T. Hayat, T. Muhammad, S.A. Shehzad, A. Alsaedi, “Three-dimensional boundary layer flow of Maxwell nano-fluid: mathematical model”, *Appl. Math. Mech*., 36 (6) 747—762, (2015).

[14]. G. K. Ramesh, B. J. Gireesha, T. Hayat, A. Alsaedi, “Thermal radiation and chemical reaction: A numerical study”, *J. Nano-fluids,* 4 100—106, (2015).

[15]. W. A. Khan, M. Khan, R. Malik, “Three-dimensional flow of an Oldroyd-B nanofluid towards stretching surface with heat generation/absorption”, *PLoS One*, 9 (8), e105107, (2014).

[16]. T. Hayat, T. Hussain, S. A. Shehzad, A. Alsaedi, “Flow of Oldroyd-B fluid with nano particles and thermal radiation”, *Appl Math Mech-Engl Ed*., 36 (1) 69—80, (2015).

[17]. S. Nadeem, R. U. L. Haq, N. S. Akbar, C. Lee, Z. H. Khan, “Numerical study of boundary layer flow and heat transfer of Oldroyd-B nanofluid towards a stretching sheet”, *PLoS One*, 8 (8) e69811, (2013).

[18]. N. A. Abu Bakar, W. M. Khairy, A. W. Zaimi, R. A. Hamid, B. Bidin, A. Ishak, “Boundary Layer Flow over a Stretching Sheet with a Convective Boundary Condition and Slip Effect”, *World Appl. Sci. J*. 17 49—53, (2012).

[19]. U. Khan, N. Ahmed, S. I. U. Khan, S. T. Mohyuddin, “Thermo-diffusion effects on MHD stagnation point a stretching sheet in a nano-fluid”, *Propul Power*, 3 151—158, (2014).

[20]. B. Rushi Kumar, “MHD boundary layer flow on heat and mass transfer over a stretching sheet with slip effect”, *Journal of Naval Architecture & Marine Engineering*, 10 (2) 16—26, (2013).

[21]. O. D. Makinde, T. Chinyoka, L. Rundora, “Unsteady flow of a reactive variable viscosity non-Newtonian fluid through a porous saturated medium with asymmetric convective boundary conditions”, *Comput. Math. Appl*., 62(9) 3343—3352, (2011).